Research Article
Volume 9:6,2022

Journal of Lasers, Optics & Photonics

ISSN: 2469-410X Open Access

Microstructural and Geometric Characteristics Investigation of Laser-Aided Direct Metal Deposition

Reza Shoja Razavi*

Department of Materials and Manufacturing Engineering, Malek Ashtar University of Technology, Tehran, Iran

Abstract

Direct Metal Deposition (DMD) is a metal deposition technique, which is well- known for high-quality and high-productivity level of fabrication. In the current economic situation with worldwide trend for developing new products, the importance of time and cost reduction increases day-by-day. To achieve this goal the man-machine-material interaction should be maximized. Direct Laser Metal Deposition (DLMD) is one of the most famous approaches for this. DLMD is one kind of 3D printing technology (additive manufacturing) together with laser cladding process. In DLMD, it is possible to fabricate fully functional metallic parts directly from CAD data, which involves a feeding of metal powders through a nozzle into a high power laser beam and creates a melt pool on the surface of the solid substrate upon which a metallic powder is injected. DLMD process are now acknowledged worldwide and is also known to all by several other names such as Laser Metal Deposition (LMD), Direct Laser Deposition (DLD), Laser Engineered Net Shaping (LENS), Direct Light Fabrication (DLF), Laser Deposition Welding (LDW) and Powder Fusion Welding (PFW). After development of this process in 1995, lot of researchers for several years work on various aspects of high quality deposition with dimensional accuracy such as good clad geometry, clad height, and microstructure study of the mechanical properties. An attempt has been made to focus on proper selection of the set up configuration for direct laser metal deposition to fulfill the requirement and help to achieve high quality deposition. Empirical-statistical models have been produced since the advent of LDMD as they avoid the complexity of analyzing the physical phenomena of the process itself. Direct metal deposition is typically described as having three “primary” process inputs of laser power, powder mass flow rate, and traverse speed. Most models have concentrated on relating these to final track geometry, typically using regression methods to relate input and response variables.

Permitting materials to grow along specific orientation by means of directional solidification technique can optimize their structural or functional properties. Ni-based super alloys are the preferred material for turbine blades given their high temperature strength, microstructural stability, and corrosion resistance. Casting methods have been improved from conventional investment casting, which produces an Equiaxed (EQ) grain structure, to Directional Solidification (DS), which produces Columnar-Grain (CG) and Single Crystal (SC) structures. Although polycrystalline Ni-based super alloys are inherently strong, their properties can be further improved through processing. Ensuring crystal cohesion during solidification by avoiding the formation of cracks and pores is a major challenge in materials science. Under others, the safety of gas turbine components and of laser welds for the aerospace and automotive industries depends on it. Solidification cracking (also called hot cracking or hot tearing) is characterized by extended openings that form during solidification in the mushy zone.

Keywords: Direct metal deposition • Powder mass flow rate • Clad height • Laser power • Traverse speed • Directional solidification • Corrosion resistance • Turbine blades

Introduction

Geometry prediction of laser clads

Laser cladding is a noble technique for surface engineering by which think protective coatings with high quality and strong metallurgical bonding can be deposited on various substrates. The process can be applied in three different implementations; using a pre-placed layer, wire feeding, and powder injection. However, using pre-placed layer and wire feeding can be time consuming, difficult to adjust and control on complex geometries, and lead to high dilution rates. The powder injection implementation is more attractive and offers the most benefits.

***Address for Correspondence:** Reza Shoja Razavi, Department of Materials and Manufacturing Engineering, Malek Ashtar University of Technology,Tehran, Iran; E-mail: shoja_r@yahoo.com*

Received: 10 Jun, 2020, Manuscript No. jlop-22-002-Pre-Qc-22; **Editor assigned:** 15 Jun, 2020, Pre QC No. jlop-22-002-Pre-Qc-22; **Reviewed:** 22 Jul, 2020, QC No. jlop-22-002-Pre-Qc-22; **Revised:** 20 Jul, 2022, Manuscript No. jlop-22-002-Pre-Qc-22; **Published:** 02 Sep, 2022, DOI: 10.37421/2469-410X.22.9.27

The laser cladding process with powder injection is operationally described in terms of three main different parameters, i.e. scanning speed V (mm/s), powder feeding rate F (mg/s), and laser power P (W). However, there are other processing parameters such as laser beam spot size, laser beam energy distribution, size and speed of powder particles, and the amount and type of carrier and shielding gas, etc. taking into consideration the overwhelming number of processing parameters and their mutual dependencies, optimization of the process is still challenging. Although several physical models have been proposed to describe the laser cladding process, empirical-statistical models can be used to avoid analyzing complex physical phenomena of the process. Therefore, empirical-statistical models of the laser cladding process with powder injection and an exploration into statistical correlations between the main processing parameters and geometrical characteristics of single clad tracks are still vital for successful deposition of functional coatings.

Materials and Methods

Most empirical-statistical models have focused on relating the main processing parameters to the final geometry of the single clad tracks, usually using some analyses based upon regression models including Analysis of Variance (ANOVA), Response Surface Methodology (RSM), and Regression Analysis (RA). Using there analyses, some researchers have experimentally investigated the empirical-statistical correlations between the geometrical characteristics and the main processing parameters for various coating/substrate combinations in the laser cladding process with powder injection. On the one hand, MCrAlY (where the M stands for Ni and/or Co) are functional and prevalent coatings that are being frequently used to protect high- temperature and high-pressure gas turbine blades and vanes made of nickel-based super alloys, Inconel 738 in particular. On the other hand, the geometrical characteristics of single clad layer (thick, dense and well-bonded) formed by overlapping single clad tracks. Therefore, most of studies aim to relate the main processing parameters to the geometrical characteristics of single clad tracks using the regression analysis method so as to propose an empirical-statistical guideline for coaxial laser cladding of MCrAlY powder on Inconel supper alloy and reduce the needs for extensive and time consuming experiments.

Developed an empirical-statistical model for coaxial laser cladding of NiCrAlY powder on Inconel 738 super alloy. In this study, an as-cast 738 super alloy with the dimension of 100 × 100 × 5 mm and NiCrAlY powder (PAC9620AM, USA) with the particle size of 50-100 μm were used as the substrate and clad powder obtained by Optical Emission Spectrometry (OES) [1]. Morphological evaluation of the powder was performed by Field Emission Scanning Electron Microscopy (FE-SEM) (SIGMA VP, ZEISS). A Coaxial laser cladding system equipped with a powder feeder with a four-way coaxial nozzle, a 700 W pulsed Nd:YAG laser and a XYZ-Rotation CNC machine was used for the experiments. In all the experiments, the laser beam was defocused on the work piece resulting in the laser beam spot diameter of 1mm. The argon with a flow rate of 20 L/min was used as a carrier and shielding gas. Other parameters of the pulsed Nd:YAG laser such as frequency, and pulse duration were fixed at 35 HZ, and 3 ms, respectively. In order to find the empirical-statistical correlations between the main processing parameters of coaxial laser cladding and the geometrical characteristics of the single clad tracks, a wide variety of processing parameters (laser power P (W), scanning speed V (mm/s) and powder feeding rate F (mg/s) were chosen, based upon a gradual increase in one individual parameter while the other parameters were kept constant.

Based on the considerations mentioned above, the processing map for the coaxial laser cladding of NiCrAlY powder on the Inconel 738 super alloy can be constructed that related geometrical characteristics of the single clad track to their applied processing parameters. Figure 1 represents such a map in terms of laser power (P) on the vertical axis and the amount of powder material delivered per unit length (F/V) on the horizontal axis. Considering the linear relation between the Dilution (D) and F/V parameter, the second horizontal axis can be derived from each combination of processing parameters. The two solid vertical lines on the processing map mark the advisable values of dilution for single clad tracks (15-25%). The shaded region on the processing map represents plausible limits to acquire free-porosity clad tracks with good metallurgical bonding to the substrate and low dilution (Figure 1).

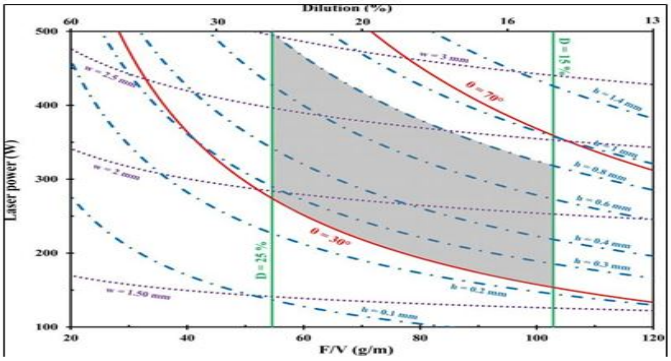

Figure 1. The processing map for coaxial laser cladding NiCrAlY powder on Inconel 738 super alloy in terms of P *vs.* F/V representation.

In another work [2], investigated the Co-Cr-Mo powder to form clads on a γ -TiAl substrate. The single track geometrical characteristics such as width, height, penetration depth, dilution and wetting angle play the important role to control the characteristics of laser clad coatings formed by overlap of individual tracks. In this research, relation between the main coaxial laser cladding parameters (laser power P, laser beam scanning speed S and powder feeding rate F) and geometrical characteristics of single tracks by linear regression analysis has been investigated. The results show that the clad height (H) depends linearly on the $FS^{-5/4}$ parameter with the laser power having a minimal effect. Similarly, the cladding width W is controlled by ye $PS^{-2/3}$ parameter. The penetration depth b and dilution (D) are proportional to $P^2S^{-1/4}F^{-1/4}$ and $P^{2/3}S^{1/2}F^{-1/2}$ respectively and wetting angle in controlled by the $P^{1/4}S^{1/2}F^{-1/2}$ parameter. These empirical dependencies are observed with high values of the correlation coefficient (R>0.9). Finally, based on these empirical relations, a laser cladding processing map for laser cladding on Co-Cr-Mo powder on TiAl substrate was designed shown in Figure 2. These can be determined a convenient prediction of the final laser clad geometry (Figure 2).

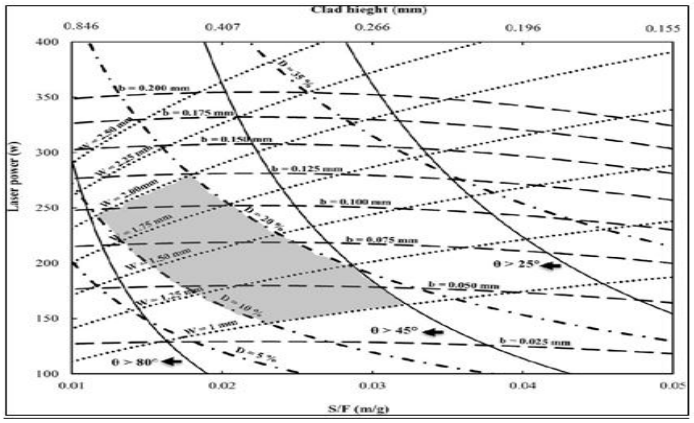

Figure 2. Laser processing map for coaxial laser cladding on Co-Cr-Mo powder on TiAl substrate in P *vs*. S/F representation.

In this study, dimension of substrate were 100 mm × 100 mm × 40 mm. Powder of Co-Cr-Mo with a mean range particle size of 45-125 μm was used. Argon was used as powder carrier gas. Laser cladding was carried out using a 0.7 kW transverse Nd:YAG laser equipped with a 4-axes CNC machine under argon shielding environment.

In another research, an empirical-statistical model for laser cladding of Ti-6Al-4V powder on Ti-6Al-4V substrate has been investigated by Razavi et al [3]. Some desirable properties of Ti-6Al-4V alloy such as low density, high specific strength, high stiffness, and good combination of mechanical and chemical properties have led this alloy to be widely used in aerospace, energy and chemistry industries. The substrate used in this study was Ti-6Al-4V alloy with the dimensions 100 mm × 100 mm × 10 mm. The nominal grain size of the powder was 90-125 μm. The samples were manufactured by laser cladding process with the following pieces of equipment: 700 W Nd:YAG laser system with a four-axes CNC machine under argon shielding environment. In this study, process optimization for laser cladding of Ti-6Al-4V alloy was performed using linear regression analysis and the following results were achieved (Figure 3).

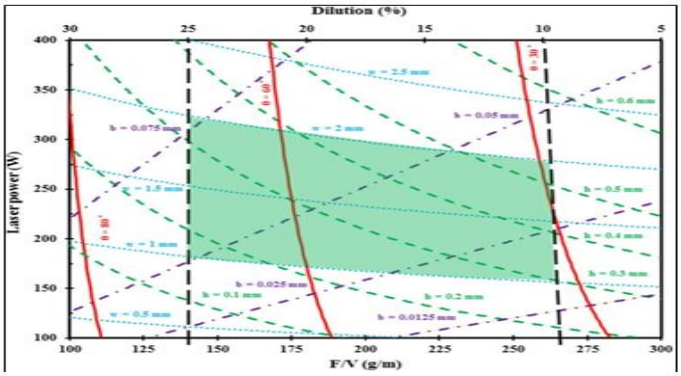

Figure 3. Processing map for laser cladding of Ti-6Al-4V alloy on the same substrate in terms of P *vs*. F/V representation.

The clad height mainly depends on laser power and laser scanning rate, while powder feeding rate was the parameter with less impact. This relation could be written in form of PV-1F2/4.

The clad width controlled by PF-1/3 combined parameter, so that powder feeding rate was a dispensable parameter.

The dilution was mainly controlled by the combined parameter as $VF^{-1/2}$, which laser power was ineffective parameter. In addition, the penetration depth was mainly proportional to $PVF^{-1/8}$.

The wetting angle was mainly controlled by the combined parameter as $P^{3/4}V^{-1}F^{-1/4}$.

A laser cladding processing map for laser cladding of Ti-6Al-4V powder on Ti-6Al-4 V substrate was designed based on the relations between the process parameters and the geometrical characteristics.

Developed an empirical-statistical model for laser cladding of WC-12Co powder on AISI 321 Stainless steel [4]. Combination of WC and Co encompasses substantial hardness and toughness together because WC benefits from a high hardness and Co is considered to be a tough material. In this study, an AISI 321 stainless steel plate with dimension of 200 mm × 200 mm × 10 mm was used as the substrate and WC-12Co powder with particle size of 15-45 μm was the clad powder material. Laser source was a 700 W pulsed Nd:YAG with a defocused laser beam of 1 mm. Argon was used as a shielding and carrier gas with flow rates of 20 L/min and 15 L/min respectively. Pulse duration and Frequency of Nd:YAG laser were 3.5 ms and 35 HZ respectively. Process optimization in coaxial laser cladding of WC-12Co powder on AISI 321 stainless steel was performed using an empirical-statistical viewpoint. The main results are as follows:

The clad height statistically depends on laser power and scanning speed while powder feeding rate was the parameter with less impact. The statistical relation could be written as $P^2V^{-2}F^{1/4}$.

The clad width was chiefly under the control of a combined parameter obtained from laser power and scanning speeds so that the rate of powder feeding was a dispensable parameter. The combined parameter for the clad width could be presented as $P^2V^{-1/2}$.

The penetration depth was proportional to the combined parameter as $P^2V^{1/4}F^{-1/4}$. However, the dilution was found to be proportional to the combined parameter as $P^{3/2}V^2F^1$.

The wetting angle was under the control of the combined parameter $V^{-1}F^2$, for which the laser power was ineffective.

The processing map was modeled on empirical-statistical relations to acquire suitable geometry and low porosity clads. A narrow processing range was noticed in the process (Figure 4).

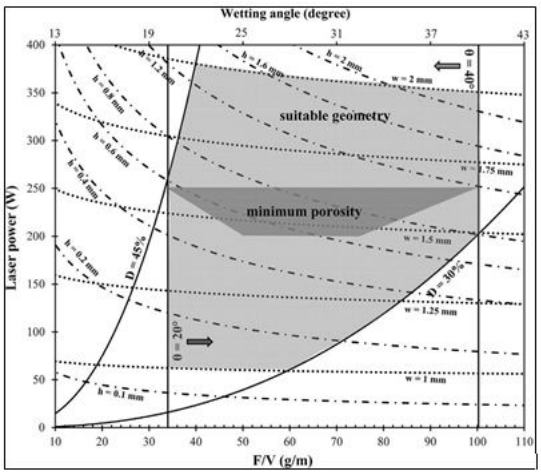

Figure 4. P *vs*. F/V depiction of processing map for laser cladding of WC-12Co powder on AISI 321 steel.

Working on an empirical-statistical model and geometric characteristics prediction for Laser-Aided Direct Metal Deposition of Inconel 718 super alloy was another research by Razavi et al [5]. Inconel 718 commercial powder was used. The powder has a spherical morphology with a grain size of 45 ± 15 μm. Inconel 718 cast super alloy was used as the substrate. Circular plates of the substrate with a diameter of 15 mm and a thickness of 5 mm were prepared. The LDMD process was performed using a 700 W pulsed Nd:YAG laser. The output of this laser have a standard square shape. Accessible parameters in this laser are frequency of 1-250 HZ, pulse width 0.25-25 ms, and pulse energy 0-70 J. According to the design of powder injection nozzle, the angle of powder injection with laser beam is 30^{o}. Argon gas was used as shielding and powder carrier gas at a rate of 20 and 15 L per minute. Laser-aided Direct Metal Deposition (LDMD) of Inconel 718 super alloy was performed and an empirical-statistical modeling was successfully developed using linear regression method (Figure 5).

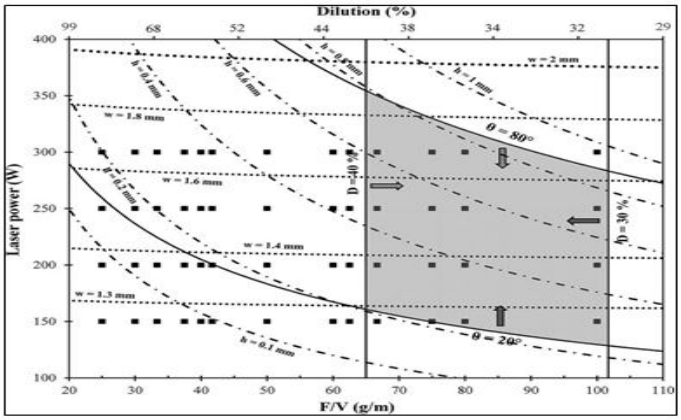

Figure 5. Process map for LDMD of Inconel 718 super alloy.

The relationship between the key process parameters and geometric characteristics of single-track deposits were determined and the following conclusions can be drawn.

The height was dependent on laser power, scanning speed, and powder feeding rate; however, the impact of laser power was more pronounced than that of scanning speed, and powder feeding rate. This relationship can be written as $P^{3/2}V^{-1}F^{1}$.

The width was precisely controlled by a combined parameter including laser power and scanning speed. Powder feeding rate had no effect and it is possible to ignore its effect. The combined parameter was obtained in the form of $P^{2}V^{-1/4}$.

The depth of penetration was proportional to the combined parameter as $P^{2}F^{-1}$. However, the dilution was proportional to $V1F^{-1}$, which is independent of laser power.

The wetting angle was controlled by the combined parameter as $P^{2}V^{-1}F^{1}$. In addition, the calculated values of the wetting angle using the width and height showed the correctness and accuracy of the measurements.

A process map was designed based on experimental relationships that could predict geometric characteristics and determine the appropriate parameters for LDMD of Inconel 718 super alloy.

In a recent research conducted by Razavi et al., microstructural evolution of laser cladding of Inconel 718 powder on A-286 substrate [6] has been done. The A-286 superalloy, a Fe-Ni-Cr austenitic Precipitation Hardening (PH) stainless steel, is notoriously susceptible to hot cracking phenomena in both the HAZ and FZ. Liquation cracking in the HAZ occurs due to the formation of eutectic Laves phase along the grain boundaries as a result of constitutional liquation of the pre-existing Ti carbides in the base material microstructure.

5 mm thick solution and aged A-286 austenitic precipitation hardening stainless steel plates were used as the base metal. The Inconel 718 gas atomized powder (MetcoClad 718) with a nominal particle size ranging from 45 to 90 μm was chosen as the powder material. The laser cladding process was conducted using a pulsed Nd:YAG laser system equipped with a powder feeder with a four way coaxial nozzle. The laser beam was defocused on the substrate to a spot size of 2 mm, which corresponded to a standoff distance of 14 mm. The other laser beam parameters such as pulse duration and frequency were kept constant at 5 ms and 35 HZ, respectively. Argon gas with the flow rate of 20 L/min was directed through the laser beam nozzle toward the melt pool as the shielding gas. Moreover, argon gas at a flow rate of 15 L/min was used to inject the powders into the laser beam as a carrier gas.

Microstructural evolution during dissimilar laser cladding of a Ni-based superalloy powder (Inconel 718) on a solution and aged Fe-based superalloy substrate (A-286) was investigated in the present paper. The primary conclusions emerging from this research are as follows:

The fusion zone microstructure mainly consists of austenitic dendrites, interdendritic laves phases, and Nb carbides at the interdendritic regions. Moreover, some small particles rich in Ti (C, N) were found in the fusion zone. Indeed, some pre-existing TiC particles in the substrate microstructure were not completely dissolved in the fusion pool during the laser cladding process but remained solid and reacted with nitrogen atoms to form these Ti (C,N) particles.

The hardness profile was featured by HAZ softening, which can be attributed to the dissolution of the γ^{0} precipitates in the austenitic matrix during the experienced thermal cycle of the laser cladding process. The HAZ softening became more severe closer to the fusion boundary, since the regions near the fusion line have a higher potential to promote γ^{0} dissolution. Moreover, the fusion zone exhibited lower hardness compared to the base metal due to the absence of strengthening precipitates (Figure 6).

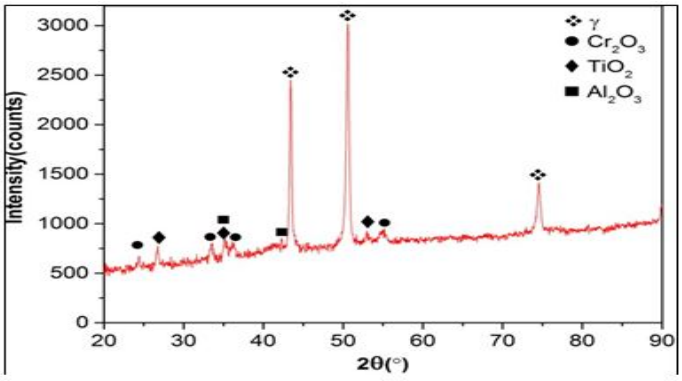

Figure 6. The X-ray diffraction pattern of the laser cladding track indexing γ, Cr_2O_3, TiO_2, and Al_2O_3 phases.The X-ray diffraction pattern of the laser cladding track indexing γ, Cr_2O_3, TiO_2, and Al_2O_3 phases.

Based on the “no-slip” boundary condition along the fusion zone boundary, as well as the lower liquidus temperature of fusion zone compared to that of the base metal, an unmixed zone in the shape of a beach and peninsula was formed.

Despite using high purity inert gas, a slag oxide layer, rich in Al and Ti, was formed on the clad surface. However, this slag oxide layer can be removed after the cladding process.

Results

Solidification cracking

The development of directional or completely equiaxed microstructures by the laser cladding process can determine the final properties and applications of Inconel 718 alloys. R.Shoja Razavi et al, have evaluated the solidification and microstructure on Inconel 718 super alloy in laser cladding [7] in a recent research. The dominant microstructure obtained by laser cladding process is columnar dendrites in the direction of . Actually, this is the preferred growth direction for the materials that are solidified with the FCC lattice. The microstructure of Inconel 718 alloy after laser cladding process is essentially consists of austenite dendrites and interdentritic lave phase.

In this study, the commercial powder of Inconel 718 with spherical morphology was used as a feeding material. The casting Inconel 718 super alloy was used as the substrate. The laser cladding process was performed using pulsed ND:YAG laser device (IQL20 model) with nominal power of 700 W in which the output pulses are square shaped. Argon gas was used as protective and carrier gas with flow rates of 20 and 15 L/min respectively. In the laser cladding process, different laser parameters were evaluated to obtain a suitable coating. The three main parameters of mean power (P), laser scanning rate (V) and powder feeding rate (F) were considered as variables.

The microstructure of the cladded layer consists of a columnar dendritic and equiaxed dendritic structure. The microstructure of the cladded layer is columnar dendritic at the laser powers of 150 W and 200 W and the structure is equiaxed dendritic at the laser powers of 250 and 300 W. In fact, by increasing the power the extent of the equiaxed zone increases.

At high laser cladding rates, the R value (the growth rate of dendrite tip) increases, resulting in a reduced G/R ratio (constitutional undercooling) and the structure tends toward an equiaxed dendritic structure. For this reason, with increasing scanning rate from 4 to 6 mm/s, equiaxed dendritic structure increases.

With increasing laser power from 150 to 300 W and laser scanning rate from 4 to 6 mm/s, the secondary arms spacing in the interface decreased from 1.08 to 0.98, and the cooling rate increased from 2.3649 × 104 to 3.2641 × 104.

In addition to the G/R ratio, a heterogeneous nucleation is also effective in creating an equiaxed dendritic structure. For this reason, with the increase of the powder feeding rate, the extent of equiaxed zone increases. However, the effect of the powder feeding rate cannot be directly and specifically determined.

The phases formed in the laser cladded sample include the Lava, Nb phases and carbide and nitride dendritic phases are formed due to the segregation of γ phase.

In another research, Shoja Razavi et al., investigated the clad bead geometry- solidification cracking relationship of laser cladding of Inconel 718 powder on a non-weldable substrate [8].

The 5 mm thick solution and aged A-286 austenitic precipitation hardening stainless steel plates were used as Base Metal (BM). The Inconel 718 Gas Atomized (GA) powder was chosen as cladding material. The nominal particle size of the Inconel 718 powders was

50-100 mm. The laser cladding process was performed by a pulsed ND:YAG laser system equipped with powder feeder with a four way coaxial nozzle. The laser beam with a Gaussian distribution energy was defocused on the substrate to a spot size of 2 mm where the standoff distance is 14 mm. The powders were fed into the laser beam by the protection of argon gas with the flow rate of 15 L/min. Moreover, argon gas with the flow rate of 20 L/min was used as shielding gas to protect the melt pool from oxidation. To study the effects of the process parameters on the formation of solidification cracking, the processing map could be implemented as a useful chart to find the feasible limits of clad geometries with no solidification cracking.
A-286 is classified as non-weldable alloy and prone to solidification

cracking, while, Inconel 718 alloy is a well-known weldable nickel base super alloy with low susceptibility to solidification cracking.

Generally, the solidification cracking occurs when sufficient thermal stresses pulling on intergranular liquid film during the last stage of fusion zone solidification. The high temperature gradient during the laser cladding process induces the thermal stresses.

The linear statistical model determined how the geometrical attributes were affected by the process parameters, and the large value of their linear regression coefficients (R>0.95) confirmed the models accuracy. The clad height, width, angle and dilution ratio are proportional.

The processing map reveals that the crack-free single laser cladding tracks were situated in the region with dilution ratio of <10%. The rationale behind this condition is to limit the detrimental effects of base metal chemical composition.

The base metal dilution ratio not only adjusted the chemical composition of the fusion zone but also controlled the segregation potential of the alloying elements. The more severe segregation of alloying elements such as Nb, Mo and Ti occurred with increasing the base metal dilution ratio. Since the A-286 base metal is an iron-based superalloy, the Fe addition to the fusion zone increased the segregation potential of Nb, Mo and Ti. Moreover, A-286 substrate could increase the content of impurity elements (S, P and B) and Ti in the fusion zone that have a strong deleterious effects on solidification cracking susceptibility.

Discussion

Prediction of solidification cracking by an empirical-statistical analysis for laser cladding of Inconel 718 powder on a non-weldable substrate was another research by Razavi et al [9]. They developed a prediction of solidification cracking during laser cladding of Inconel

718 powder on A-286 Fe- based super alloy with empirical-statistical approach. During cladding, fusion welding or fusion-based additive manufacturing, solidification cracking may occur in a wide range of key engineering alloys such as AISI 310 stainless steel and Ni-based super alloys.

In this work, Inconel 718 was deposited on a 5 mm thick solution treated (heat treated at 980°C for 1 hr followed by cooling in oil) A-286 austenitic precipitation hardening stainless steel substrate. The Inconel 718 Gas Atomized (GA) powder had a nominal particle size ranging 45-90 μm. Laser cladding was performed using a pulsed Nd:YAG laser system (400 W maximum power, λ =1064 nm) equipped with a powder feeder with a four way coaxial nozzle. The laser beam, had a Gaussian distribution of energy and was defocused on the substrate to a spot size of 2 mm at a standoff distance of 14 mm. Argon gas with a flow rate of 20 L/min was directed through the laser beam nozzle toward the melt pool as the shielding gas to protect the melt pool from oxidation. Moreover, another argon gas jet at a flow rate of 15 L/min was used to inject the powders into the laser beam path.

The linear statistical model determined how the geometrical attributes were affected by the process parameters. The large values (approaching unity) of the correlation coefficients, $R \geq 0.97$, associated with randomly scattered residuals shows a good correlation between the physical attributes of the laser cladding tracks and the combined process parameter and it endorses the linear statistical models. The clad height, width, angle and dilution ratio are proportional.

Accordingly, the higher laser powers with the different degrees of magnitude 2, 1.5 and 0.5 forms a thicker and wider clad layer with the larger clad angle. However, the higher laser power provides a clad layer with a lower dilution ratio since it has a weak inverse degree of magnitude, -0.25. Moreover, the positive degrees of magnitude 2 and 1 for the F/V ratio of clad height and angle, respectively, result in the formation of a thicker layer with the larger clad angle by increasing the F/V ratio. However, the clad width and substrate dilution ratio decrease by a higher F/V ratio because of the degree of magnitude -0.5.

Conclusion

The processing map reveals that the substrate dilution ratio is the critical geometrical feature to avoid solidification cracking, since the crack-free single laser cladding tracks were situated in the region with dilution ratio below 25%. Indeed, the solidification cracking would not occur when the laser cladding parameters were adjusted to the levels which deposit a track satisfying the substrate dilution ratio condition.

The base metal dilution ratio not only adjusted the chemical composition of the fusion zone but also controlled the segregation potential of the alloying elements. The more severe segregation of alloying elements occurred by increasing the base metal dilution ratio. Moreover, the Scheil-Gulliver solidification simulation revealed that higher substrate dilution ratio is accompanied by wider solidification temperature range and thus, higher susceptibility to solidification cracking. Therefore, the rationale behind the limitation of substrate dilution level (D<25%) is to reduce the detrimental effects of the substrate chemical composition in solutes redistribution and STR widening.

References

1. Ansari, M, Razavi RS and Barekat M. “An empirical-statistical model for coaxial laser cladding of NiCrAlY powder on Inconel 738 superalloy.” *Opt Laser Technol* 86 (2016):136-144.
2. Barekat, M, Razavi RS and Ghasemi A. “Nd: YAG laser cladding of Co–Cr–Mo alloy on γ-TiAl substrate.” *Opt Laser Technol* 80 (2016):145-152.
3. Nabhani, M, Razavi RS and Barekat M. “An empirical-statistical model for laser cladding of Ti-6Al-4V powder on Ti-6Al-4V substrate”. *Opt Laser Technol* 100 (2018):265-271.
4. Erfanmanesh, M, Abdollah-Pour H, Mohammadian-Semnani H and Shoja-Razavi R. “An empirical-statistical model for laser cladding of WC-12Co powder on AISI 321 stainless steel.” *Opt Laser Technol* 97 (2017):180-186.
5. Jelvani, S, Shoja Razavi R, Barekat M and Dehnavi M. “Empirical-statistical modeling and prediction of geometric characteristics for laser-aided direct metal deposition of inconel 718 superalloy.” *Met Mater Int* 26 (2020):668-681.
6. Alizadeh-Sh, M, Marashi SP, Ranjbarnodeh E and Shoja-Razavi R, et al. “Dissimilar laser cladding of Inconel 718 powder on A-286 substrate: Microstructural evolution..” J. Laser Appl. 32(2020):22-48.
7. Jelvani, S, Razavi RS, Barekat M and Dehnavi MR et al. “Evaluation of solidification and microstructure in laser cladding Inconel 718 superalloy”. *Opt Laser Technol* 120 (2019):105761.
8. Alizadeh-Sh, M, Marashi SP, Ranjbarnodeh E and Shoja-Razavi R. “Laser cladding of Inconel 718 powder on a non-weldable substrate: Clad bead geometry-solidification cracking relationship.” *J Manuf Process* 56 (2020):54-62.
9. Alizadeh-Sh, M, Marashi SP, Ranjbarnodeh E and Shoja-Razavi R, et al. “Prediction of solidification cracking by an empirical-statistical analysis for laser cladding of Inconel 718 powder on a non-weldable substrate.” *Opt Laser Technol* 128 (2020):106-107.

How to cite this article: Razavi Reza Shoja., "Microstructural and Geometric Characteristics Investigation of Laser-Aided Direct Metal Deposition". *J Laser Opt Photonics* 9 (2022):027